

**Research Article****S-GLUTATHIONYLATION OF CYSTEINE-217 ALLOSTERICALLY INHIBITS TRIOSE-PHOSPHATE ISOMERASE: A MOLECULAR DYNAMICS STUDY****M. S. Shahul Hameed***School of Life Sciences, B.S.Abdur Rahman University, Chennai 600048, India*

**Abstract:** Reversible S-glutathionylation is an important post-translational modification of proteins involved in redox signaling under normal physiological conditions and plays a protective role during oxidative / nitrosative stress by preventing irreversible oxidation of cysteine residues in proteins. Several enzymes of the glycolytic pathway have been shown to be targets of S-glutathionylation, wherein S-glutathionylation results in inhibition of the pathway. In this study the effects of S-glutathionylation of Triose-phosphate Isomerase are reported. The effect of S-glutathionylation on the structure and dynamics of TIM were examined through molecular dynamics simulations. MD simulation study has provided interesting insights into a novel mechanism of allosteric regulation of this enzyme by S-glutathionylation of Cysteine-217 in Helix G. The simulations predict that S-glutathionylation of Cys-217 leads to a complete loss of active site loop structure and causes alterations in its dynamics. This leads to premature substrate dissociation from active site leading to enzyme inhibition.

**Keywords:** Protein S-Glutathionylation; metabolic regulation; triose-phosphate isomerase; Molecular Dynamics simulations; allosteric inhibition.

**Introduction**

S-Glutathionylation is an important post-translational modification of protein cysteine residues. It generally rises during oxidative / nitrosative stress but might also rise in unstressed cells under normal physiological conditions. Studies suggest that S-glutathionylation regulates a variety of cellular processes by modulating protein function and also plays a protective role by preventing irreversible oxidation of protein thiols (Klatt *et al.*, 2000; Cooper *et al.*, 2011; Xiong *et al.*, 2011; Mieyal *et al.*, 2012). Proteomics based studies have identified many target enzymes including glycolytic enzymes, protein kinases, transcription factors, Ras proteins, heat shock proteins, ion channels and pumps, mitochondrial

proteins and cytoskeletal proteins (Ghezzi *et al.*, 2005).

Dramatic reversible changes in cellular metabolism can occur due to reversible glutathionylation of key metabolic enzymes. Glycolytic enzymes like glyceraldehyde-3-phosphate dehydrogenase, enolase, aldolase, phosphoglycerate kinase, pyruvate kinase and Triosephosphate isomerase have been confirmed to be targets of S-glutathionylation (Mohr *et al.*, 1999; Cotgreave *et al.*, 2002; Fratelli *et al.*, 2002; Ito *et al.*, 2003; Michelet *et al.*, 2006; Dalle-Donne *et al.*, 2009). Triose-phosphate isomerase (TIM) which catalyzes the interconversion of triose-phosphates, glyceraldehyde 3-phosphate and dihydroxyacetone phosphate, has been well characterized both structurally and kinetically (Albery *et al.*, 1976; Knowles *et al.*, 1991). The dynamics of this enzyme has been thoroughly characterized both during the resting state and during active catalysis (Rosovsky *et al.*, 2001; Cui

Corresponding Author: M. S. Shahul Hameed  
E-mail: shahulhambiotech@gmail.com

Received: March 28, 2016

Accepted: June 9, 2016

Published: June 12, 2016

*et al.*, 2002; Kurkcuoglu *et al.*, 2006). The enzyme is active only as a dimer although each monomer has its own catalytic residues (Waley *et al.*, 1973; Zabori *et al.*, 1980; Zomosa *et al.*, 2003). Inhibition of TIM by S-glutathionylation has been reported in *Arabidopsis thaliana* and yeast (Ito *et al.*, 2003; Marino *et al.*, 2010) and recent studies in my lab have established the relationship between site specific glutathionylation and activity. The solvent accessibility and the  $pK_a$  value of the cysteine residues are major determinants of the susceptibility of thiols to redox regulation (Kiley *et al.*, 2004). Several independent studies have ascertained the fact that a single cysteine modification can regulate protein function at various levels like enzyme activity and protein-protein interactions (Garza-Ramos *et al.*, 1996; Nakamura *et al.*, 1997; Rhee *et al.*, 2005; D'Autreux *et al.*, 2007; Reddie *et al.*, 2008; Brandes *et al.*, 2009; Foster *et al.*, 2009; Kumsta *et al.*, 2009; Leitner *et al.*, 2009). Chemical modification of the dimeric interface cysteine present in loop1 of some homologous TIMs by thiol reagents induces drastic changes in the quaternary (subunit dissociation) and tertiary structure which leads to abolition of catalytic activity (Garza-Ramos *et al.*, 1996). For those homologous TIMs which possess Cys-217 at the N-terminal of helix G, but lack the dimeric interface cysteine (Cys-13 in loop 1), inactivation with thiol modifying reagents is achieved by local structural perturbation without any involvement of dimer dissociation (Garza-Ramos *et al.*, 1996). This suggests a possible communication between the region of the derivatized cysteine (Cys-217) and the catalytic site. Some examples of such homologous TIMs include mammalian TIMs like human TIM and rabbit TIM. TIMs from certain parasite, plant and plant fungi species have been found to possess cysteines at both Cys13 and Cys217 (Figure 1). Examples of such homologous TIMs are found in species like *Arabidopsis thaliana*, *Zea mays*, *Secale cereale*, *Plasmodium falciparum* etc.

*Plasmodium falciparum* TIM contains four cysteine residues at positions 13, 126, 196 and 217 in each sub unit. Cys13 is present on loop at the interface and lies very close to the active site residues - Lys12, His95 and Glu165. Cys126 is located on  $\alpha$ -strand 4, whereas Cys196 and Cys217 are found on helix F and helix G, respectively of

the TIM barrel (Maithal *et al.*, 2002). (Table 1). In this study S-Glutathionylation of either Cys-13 and/or Cys-217 of PfTIM has been shown to inhibit the enzyme. The mechanistic basis of allosteric inhibition of homologous TIMs, which possess Cys-217 in Helix-G, has been explained using Molecular Dynamics simulations. Further this study also sheds light on enzyme inactivation by dimer dissociation brought about by S-Glutathionylation of dimeric interface Cys-13.

## Materials and Methods

### Surface accessibility calculations

The program NACCESS (Lee *et al.*, 1971) version 2.1.2 was used to calculate the relative surface accessibility using a probe radius of 1.4 Å water molecule.

### Molecular Dynamics Study

#### Starting structure of Cys13 and Cys217 glutathionylated PfTIM

Crystal structure of closed loop conformation of wild type PfTIM (PDB ID: 1LYX) was obtained from the Protein Data Bank. The histidine residues were treated as protonated at their N<sup>8</sup> position. All other residues were assumed to be in their standard protonation states at neutral pH. The structure of glutathionylated PfTIM was generated by attaching the coordinates of glutathionylated cysteine of glutaredoxin (PDB ID: 1B4Q) to the Cys13 and Cys217 of PfTIM by overlapping the C<sup>α</sup>-C<sup>β</sup>-S<sup>γ</sup> atoms using the DeepView Swiss-PdbViewer v4.0.1. The coordinates of glutathionylated cysteine (CysSSG) was taken and processed using antechamber program of AMBER 9 and gaussian 03 (Gaussian, Inc) to prepare the necessary parameter and

**Table 1**  
Relative surface accessibility of cysteine residues in PfTIM

Residues	All-atoms	Side chain	Main chain	Non-polar	All-polar
Cys13	0.1	0.15	0.0	0.15	0.0
Cys126	0.0	0.0	0.0	0.0	0.0
Cys196	28.45	15.1	62.85	18.95	53.95
Cys217	3.6	5.0	0.00	4.95	0.0

library files for input to tleap module of AMBER 9. Force field parameterizations were carried out with HF/6-31G\* RESP charges calculated using Gaussian03. *In silico* glutathionylation was done only for Cys13 / Cys217 in subunit A. The cysteines in the other subunit were left free. Similarly for the PGA ligand, Gaussian03 was used to calculate the charges at Hartree-Fockee level of theory using 6-31G basis sets.

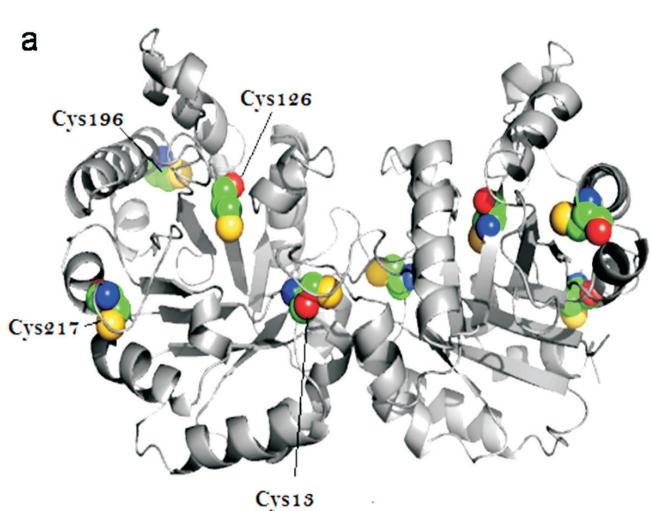
### Simulation Details

Molecular Dynamics simulations were performed using the sander module of AMBER 9 software package with the ff99 force field parameters. ff99 was originally developed for organic and biological molecules using the restrained electrostatic potential (RESP) approach to derive the partial charges. This force field is suitable for simulations of glutathionylated triosephosphate isomerase as glutathione itself is a peptide. All simulations were done on the homodimeric, loop closed *Plasmodium falciparum* triosephosphate isomerase (Parthasarathy *et al.*, 2002). However the starting structures for the different runs differ with respect to the site of glutathionylation. While

molecular system 1 used unglutathionylated starting structure (PDB ID: 1LYX), molecular system 2 used starting structure which was *in silico* glutathionylated at Cys13 (subunit A) and it will be denoted as PfTIMC13(A)-SSG. Similarly molecular system 3 used a starting structure which was *in silico* glutathionylated at Cys217 (subunit A) and it will be denoted as PfTIMC217(A)-SSG. All runs were done for a time period of at least 50 nanoseconds. The simulation details are summarized in Table 2. A periodic truncated octahedron box was used for solvation of the protein in explicit TIP3P water molecules. The molecular systems were neutralized with Na<sup>+</sup> ions. The initial solvated structures were first subjected to 200 steps steepest descent energy

**Table 2**  
Details of MD Simulations

System	Box dimension (Å)	Total no. of atoms	No. of water molecules	No. of Na <sup>+</sup> ions
Unmodified PfTIM	107	61,468	8229	12
PfTIMC13(A)-SSG	107	63,031	8379	13
PfTIMC217(A)-SSG	107	61,465	7857	13



b	13
MARKYFVAANWKCNGTLESI	<i>Plasmodium falciparum</i>
MARKFFVGGNWKCNGTAEEV	<i>Arabidopsis thaliana</i>
MARKFFFVGGNWKCNGTSEEV	<i>Ricinus communis</i>
MGRKFFFVGGNWKCNGTTDQV	<i>Sorghum bicolor</i>
MARKFFFVGGNWKCNGTTDQV	<i>Solanum tuberosum</i>
MGRKFFFVGGNWKCNGTTDQV	<i>Zea mays</i>
KFFFVGGNWKCNGTKDSV	<i>Oryza sativa</i>
MGRKFFFVGGNWKCNGTVSQV	<i>Secale cereale</i>
MGRKFFFVGGNWKCNGTVEQV	<i>Triticum aestivum</i>
RKFFFVGGNWKMNGRKQSL	<i>Homo sapiens</i>

c	217
YGGSVNTENCSSLIQQEDI DGF	<i>Plasmodium falciparum</i>
YGGSVNGGNCKELGGQADVDGF	<i>Arabidopsis thaliana</i>
YGGSVTATNCKELAAQPDVDGF	<i>Ricinus communis</i>
YGGSVTAANCCKELGAQPDVDGF	<i>Sorghum bicolor</i>
YGGSVSGANCKELAGQPDVDGF	<i>Solanum tuberosum</i>
YGGSVTAANCCKELAAQPDVDGF	<i>Zea mays</i>
YGGSVNAANCACELAKKEDIDGF	<i>Oryza sativa</i>
YGGSVNAANCACELAKKEDIDGF	<i>Secale cereale</i>
YGGSVTGTGASCKELAAQPDVDGF	<i>Triticum aestivum</i>
YGGSVTGTGATCKELASQPDVDGF	<i>Homo sapiens</i>

**Figure 1:** Cysteine residues in *Plasmodium falciparum* triosephosphate isomerase.

- Cartoon representation of dimeric PfTIM showing the position of the cysteine residues. Cysteine residues (shown in sphere representation) of only monomer A have been labeled.
- and c. Select portions of the sequence alignment of homologous TIMs which have high degree of sequence identity with PfTIM (with the exception of human TIM).

minimization, whereas the solute atoms, including the protein, were restrained by a harmonic potential with a force constant of 100.0 kcal/mol/Å<sup>2</sup>. After the initial solvent minimization, the whole system was minimized using 200 steps of steepest descent minimization without harmonic restraints. The minimized structures were then subjected to an equilibration protocol in which the temperature of the systems were gradually raised from 100K to 300K over a 10ps period while holding both the volume and temperature constant, followed by another 10ps at 300K by holding the temperature and pressure constant while allowing the volume to change for adjusting solvent density. The initial velocities were randomly assigned from a Maxwellian distribution at 100K. At the end of the equilibration, the average temperature of the final 5ps was 300K, and the average density was 1.0 g/ml. Long range electrostatic interactions were treated with the particle mesh Ewald method. Periodic boundary conditions were applied via both nearest image and the discrete Fourier transform implemented as part of the particle mesh Ewald method. All bonds involving hydrogen atoms were restrained using the SHAKE algorithm with time steps of 2fs to be taken. Global translation and rotation of the system (solvent and solute) was removed every 100 integration steps during the simulation. The initial 20ps stage was designed to equilibrate those particles that were added during the initial model-building process, including water molecules and hydrogen atoms, and to allow the systems to be solvated adequately. The initial 20ps trajectories were discarded and were followed by the production stage in which both pressure (1.0 atm) and temperature (300K) were held constant by Berendsen's coupling scheme.

The Essential dynamics of TIM was extracted from the MD simulation trajectories using the P traj module of AMBER 9. Covariance matrices were generated and analyzed by principal component analysis. The Covariance matrices were formed based on the C<sup>α</sup> atom coordinates of the residues after removal of translational and rotational motions of the protein by aligning each snapshot onto the initial conformation. Hydrogen bonding analysis for the entire length of the simulation was done using the P traj module of

AMBER 9 using default hydrogen bond parameters.

## Results

### *Molecular dynamics simulations*

To provide mechanistic insights into the inhibition of *Plasmodium falciparum* Triosephosphate isomerase by glutathionylation of Cys217, MD simulations were carried out for each of the three species of *Plasmodium falciparum* triosephosphate isomerase — unmodified PfTIM, PfTIM glutathionylated at Cys13 (PfTIMC13(A)-SSG) and PfTIM glutathionylated at Cys217 (PfTIMC217(A)-SSG). The global RMSD of the C<sup>α</sup> atoms for unmodified PfTIM was well within 2.5 Å throughout the simulation time period indicating a stable trajectory. Since non-equilibrated energy minimized structures were used as reference a initial jump in RMSD is observed for all simulations. The jumps in RMSD can be removed if the first frame from the production run trajectory (completely equilibrated structure) is used as reference for RMSD calculation. The global RMSD of the C<sup>α</sup> atoms for PfTIMC217(A)-SSG, after an initial increase, remains stable from 15ns till the entire length of the simulation, well within 3.0 Å indicating mild structural changes to the overall structure of PfTIM as a result of glutathionylation of Cys217 (Figure 2a). Running the simulations beyond 50ns showed no noticeable upward trend indicating that there is no major conformational transition after 50ns. The equilibration was achieved within a nanosecond. Changes in RMSD near 15ns time scale are due to ligand release.

### *Structural effects of glutathionylation of Cys217*

In the simulations Helix G (residues 217-222) situated just after loop 7 undergoes extensive helix transitioning and shortening in PfTIMC217(A)-SSG compared to unmodified PfTIM (Figure 2b). After 10ns of simulation run, Helix G becomes shortened and remains as a four membered 3<sub>10</sub> helix throughout the entire length of the simulation (Figure 2c and Figure 2d).

### *Loop 6 dynamics*

To probe the effect of glutathionylation of Cys217 on the loop 6 stability, hydrogen bonds which

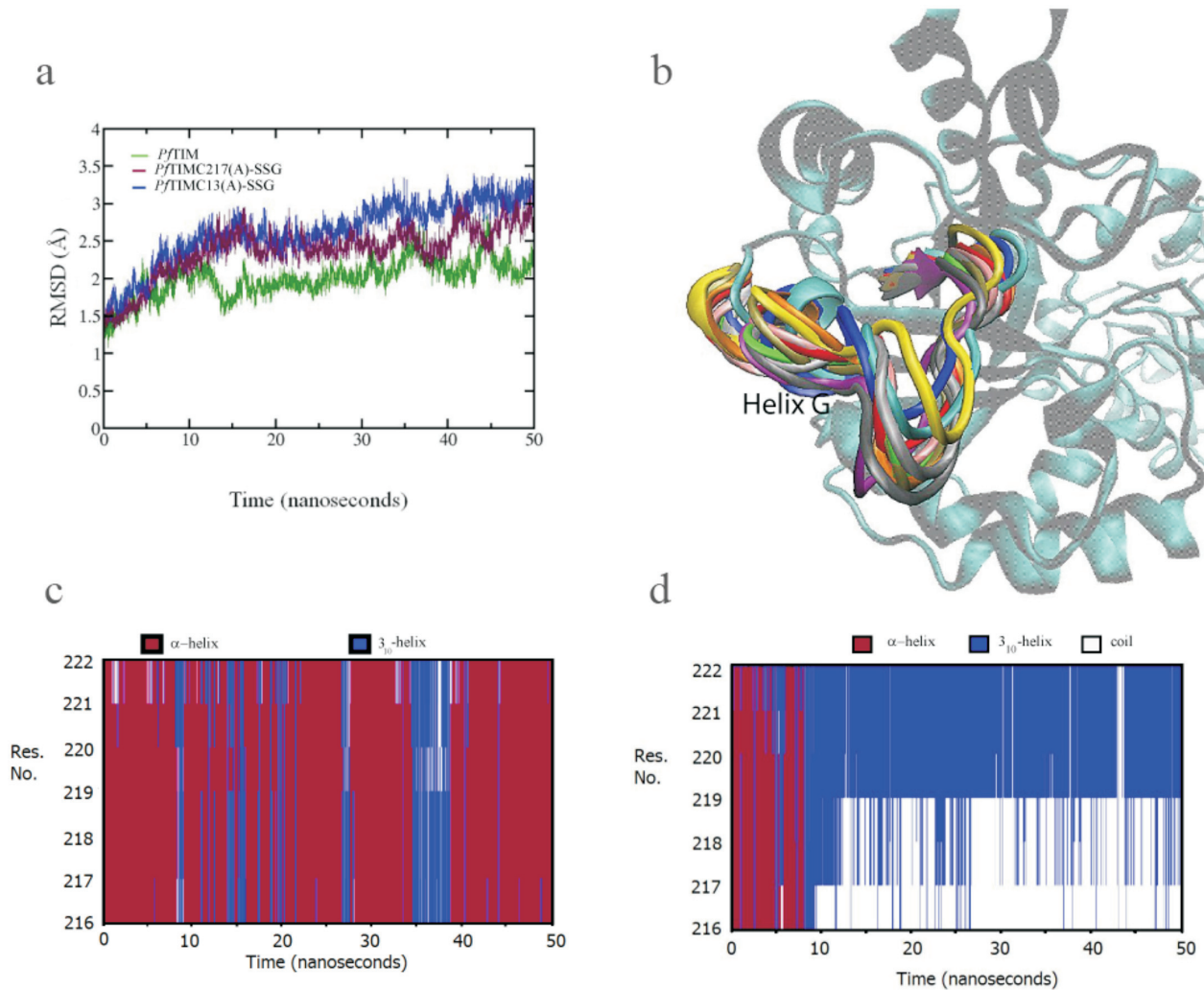


**Figure 2: MD simulations show the effect of Cys217 glutathionylation on Helix G**

- MD simulation of *in silico* glutathionylated PftIM. Root mean square deviation (RMSD) of the C<sup>α</sup> atoms for unmodified PftIM (shown in green), PftIMC13(A)-SSG (blue) and PftIMC217(A)-SSG (maroon) with respect to their minimized structure.
- Several snapshots of Helix G conformations obtained from simulations of PftIMC217(A)-SSG superposed on the starting X-ray structure shown in cyan color. (PDB ID: 1LYX).
- Select portion of DSSP plot made using simulaid program showing helix transitioning of helix G (217-222) as function of time for the 50ns trajectory of PftIM and (d) PftIMC217(A)-SSG. (α-helix is represented in red lines and 3<sub>10</sub> helix in blue lines while uncolored ones represent coil).

stabilize the loop 6 conformation, in the X-ray structures, were monitored during the simulation for the three forms of PftIM. Intraloop hydrogen bonds from the backbone amide nitrogens of Ala169 and Ile170 to the carbonyl groups of Pro166 and Val167 respectively, and from the hydroxyl group of Thr172 to the amide nitrogen of Leu174 and to the carbonyl of Trp168, which stabilize the loop structure, were monitored for a time period of 60ns. While loop 6 of unmodified PftIM and PftIMC13(A)-SSG exhibited similar characteristics and appear to be stable,

PftIMC217(A)-SSG was remarkably different and appears to be completely destabilised (Figure 3a and Figure 3b and Table 3). The intraloop hydrogen bond between the side chain of Thr172 and the carbonyl group of Trp168 was retained for an appreciable percentage of time in simulations for all three forms of the protein. The intraloop hydrogen bond between the backbone amide nitrogen of Ala169 to the carbonyl group of Pro166 was retained > 90% of the time for unmodified and PftIMC13(A)-SSG, but it was almost immediately lost and not observed during

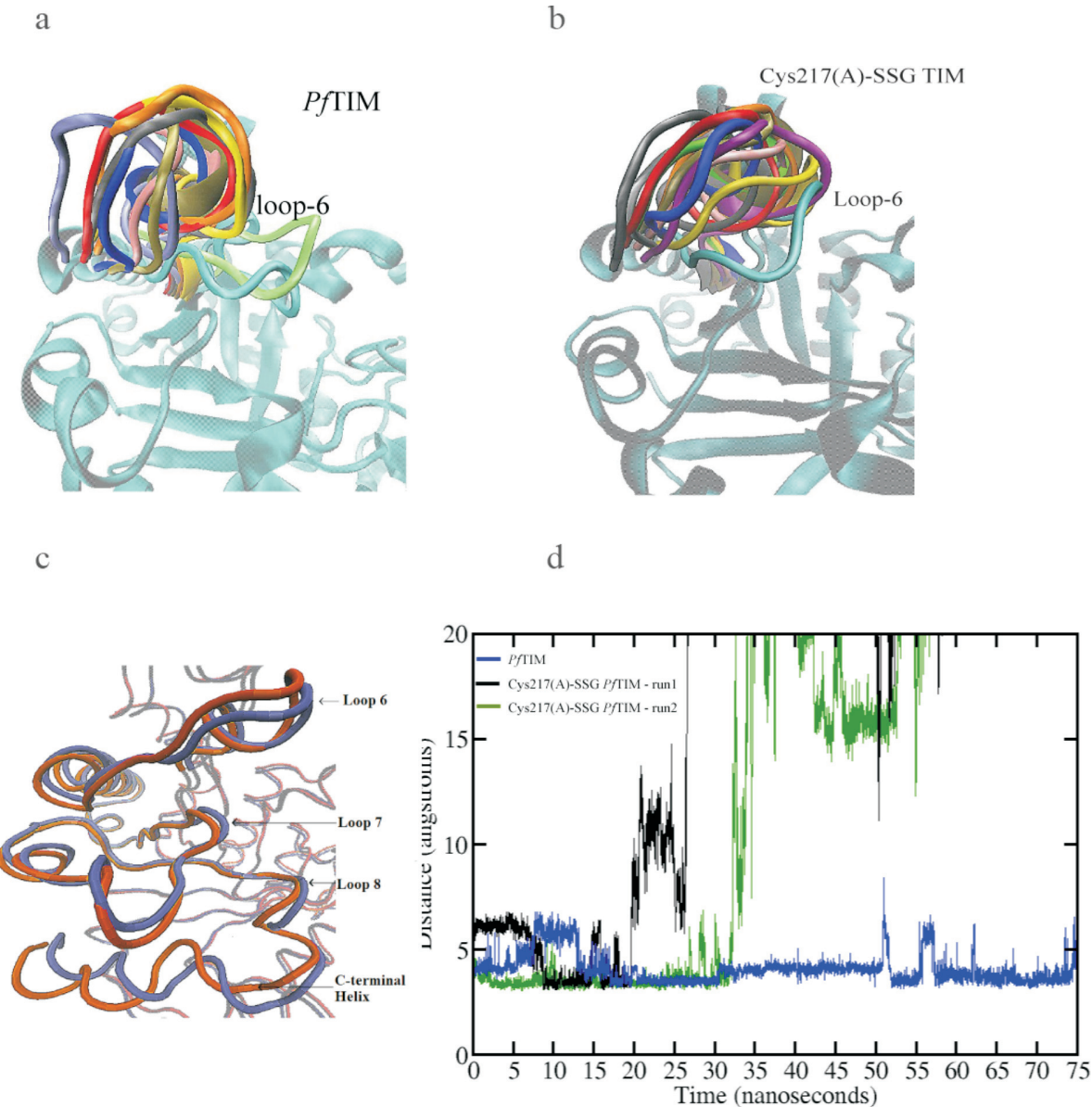


**Figure 3: Mechanism of inhibition of TIM by S-glutathionylation of Cys217 (from MD Simulations)**

- Several snapshots of loop 6 conformations obtained from simulations of unmodified PfTIM superposed on the starting X-ray structure shown in cyan color. (PDB ID: 1LYX).
- Several snapshots of loop 6 conformations obtained from simulations of PfTIMC217(A)-SSG superposed on the starting X-ray structure shown in cyan color. (PDB ID: 1LYX).
- Essential dynamics of PfTIMC217(A)-SSG - Motions of the PfTIMC217(A)-SSG along the top eigen mode. Blue and brown ribbons represent the conformations for the extreme values of the top eigenvector.
- Ligand Dissociation from the active site - Distance between the active site residue Lysine Nae atom and the phosphorous atom of the phosphate group of the ligand PGA for PfTIMC217(A)-SSG and unmodified PfTIM.

the entire length of the simulation for PfTIMC217(A)-SSG. Similarly intraloop hydrogen bonds from the backbone amide nitrogens of Ile170 and Lys174 to the carbonyl group of Val167 and the sidechain hydroxyl group of Thr172 were immediately lost and not observed during the

entire length of simulation for PfTIMC217(A)-SSG.

The hydrogen bonds which are signatures of the closed states i.e. the hydrogen bond from the backbone amide nitrogens of Gly173 and Ala176 to the hydroxyl groups of Ser211 and Tyr208 were

broken during the simulations for all three forms of the protein. During the simulations, indole ring of Trp168 samples both open and closed conformations, forming a hydrogen bond with its side chain nitrogen to the hydroxyl group of Tyr164 and the carboxyl group of Glu129. While the latter appear to stabilize closed loop state the former stabilizes the loop open state. From Table 3 it can be inferred that loop 6 is stabilized in loop open state for a very significant amount of time, by the hydrogen bond from Trp168 to Tyr164, for both unmodified and PfTIMC13(A)-SSG.

However for PfTIMC217(A)-SSG, loop 6 was stabilized by this hydrogen bond for less than 5% of the time.

These hydrogen bond statistics leads us to an interesting prediction that glutathionylation of Cys217 may allosterically induce loop 6 disorder.

### Ligand Dissociation

The essential dynamics of PfTIMC217(A)-SSG shows significant displacements for C-terminal helix and phosphate binding regions like loop 8

**Table 3**  
MD statistics of the intraloop and interloop hydrogen bonds involving loop 6.

Donor atoms	Acceptor atoms	% occurrence in PfTIM	% occurrence in PfTIMC13(A)-SSG	% occurrence in PfTIMC217(A)-SSG
169Ala, N	166Pro, O	93.4%	97.8%	-
170Ile, N	167Val, O	13.1%	30.2%	-
174Lys, N	172Thr, O <sup>γ1</sup>	32.1%	12.5%	-
172Thr, O <sup>α1</sup>	168Trp, O	79.3%	72.3%	67.5%
168Trp, N <sup>δ1</sup>	164Tyr, O <sup>η</sup>	67.1%	78.2%	4.8%
168Trp, N <sup>δ1</sup>	129Glu, O <sup>ε1</sup>	31.1%	26.2%	4.8%
173Gly, N	211Ser, O <sup>γ</sup>	2.1%	-	-
176Ala, N	208Tyr, O <sup>η</sup>	8.7%	6.6%	-

in the glutathionylated subunit along the top eigenmodes (Figure 3c). This may indicate decrease in binding affinity of the ligand for the active site leading to increased ligand dissociation and therefore may result in higher  $K_m$ . When the distance between the active site residue Lys12 N $\zeta$  atom and the phosphate group of the ligand were plotted as a function of time it was observed that for the unmodified form of PfTIM the PGA ligand does not dissociate from the active site throughout the simulation time period of 75ns. However for simulation runs done in duplicate involving PfTIMC217(A)-SSG it was observed that the PGA ligand dissociates and enters the bulk solvent in both the runs (at 20ns in run 1 and 32ns in run 2) (Figure 3d). This observation leads us to the conclusion that glutathionylation of Cys217 may decrease the binding affinity of the ligand for the active site.

### Structural effects of glutathionylation of Cys13

In spite of its negligible surface accessibility, Cys13 is an important target for S-thiolation. The

enhanced reactivity of Cys13 may be attributed to local dynamics at the interface and the electrostatic steering of negatively charged moieties due to positive electrostatic potentials contributed by Lys12 and Lys237. Figure 4 shows the important changes occurring during the course of simulations for PfTIMC13(A)-SSG.

### Effects on Dimer Stability

In a previous study it has been shown that carboxymethylation of dimer interface residue Cys13 using iodoacetamide causes dimer dissociation leading to enzyme inhibition (Maithal *et al.*, 2002). However in the present study it was observed that there was no significant precipitation upon glutathionylation of PfTIM. However treatment of glutathionylated wild type enzyme with reducing agents like DTT did not lead to reactivation of the enzyme while C13E mutant PfTIM gets reactivated. This clearly suggests that glutathionylation of Cys13 may cause structural perturbations which may not be immediately reversible.

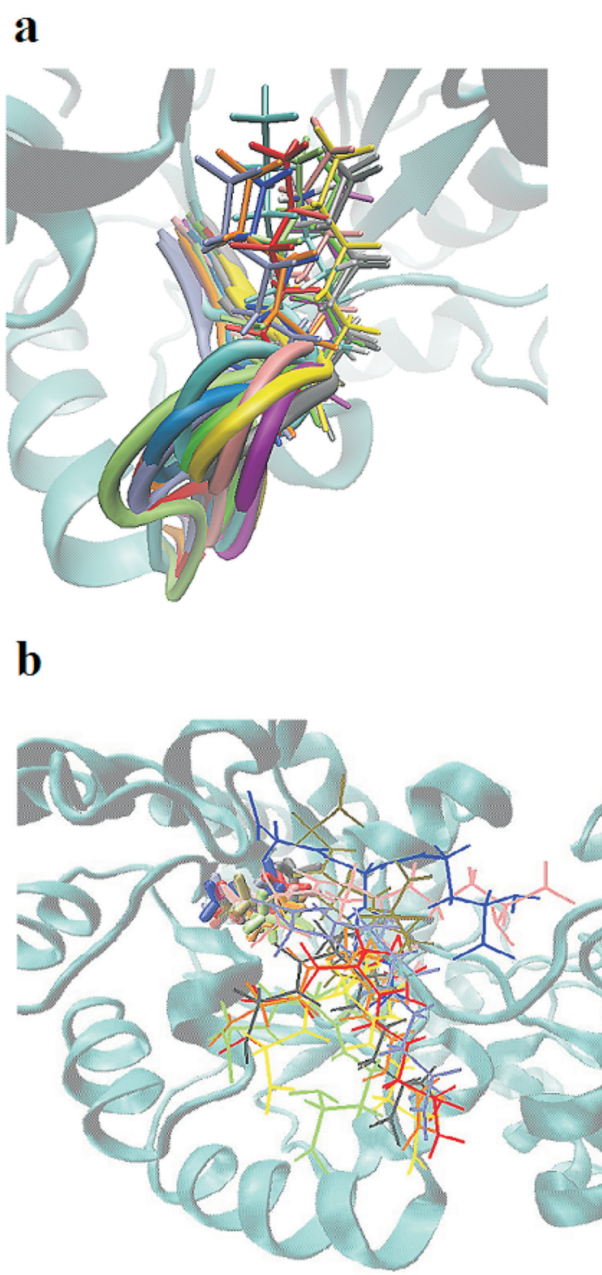


**Figure 4: MD simulations show the effect of Cys-13 glutathionylation on Loop 1**

Several snapshots of loop conformations obtained from simulations of PfTIMC13(A)-SSG superposed on the starting X-ray structure shown in cyan color.(PDB ID: 1LYX).

- a. loop 1 conformations from the A chain of the dimer (glutathionylated subunit) showing Lys12 (licorice)
- b. conformations of glutathione moiety (shown as lines) and PGA (in licorice)

The dimer interface is stabilised in PfTIM by a number of polar and non polar interactions involving loop 1 residues from one subunit to the loop 3 residues from the other subunit. Cys13 in

loop 1 forms a number of interactions with loop 3 residues of the other subunit involving the backbone of Phe69, Asn71, Gly72, Ser73, Tyr74 and Glu77. The side chain-side chain interactions are observed between Cys13 and Ser67, Glu77 and Ser79. An inter-subunit salt bridge between Glu77 and Arg98 has also been observed. Among the non-polar interactions that stabilize the dimer, a relatively large hydrophobic patch is observed at the interface of TIM. This hydrophobic patch is formed by residues Leu17, Val44 and Val46 of one subunit and Ile63, Val78, Ile82, Ala83, Leu86 and Ile88 of the adjacent subunit.

To probe the effect of glutathionylation on the stability of the dimeric interface we have analyzed the hydrogen bonding interactions over a period of 70ns. Table 4 shows the list of donor and acceptor pairs involved in hydrogen bond formation across the dimer interface in the X-ray structure and their percentage occurrence during the entire length of the simulations of PfTIM and PfTIMC13(A)-SSG. Comparing the percentage occurrences of these hydrogen bonds across the trajectories from simulations involving PfTIM and PfTIMC13(A)-SSG it is clear that with the exception of one or two hydrogen bonds there seems to be a significant difference in the

**Table 4**  
**MD statistics of native inter-subunit donor-acceptor pairs of hydrogen bonds.**

Donor atoms	Acceptor atoms	% occurrence in PfTIM	% occurrence in PfTIMC13 (A)-SSG
Asn10(A), N <sup>δ2</sup>	Thr75(B), O <sup>γ1</sup>	95.2	51.7
Cys13(A), N	Gly72(B), O	27.5	10.7
Gly72(B), N	Cys13(A), O	36.2	18.4
Gly76(B), N	Gln64(A), O <sup>ε1</sup>	96.0	10.53
Gly72(A), N	Cys13(B), O	95.6	92.2
Cys13(B), N	Gly72(A), O	58	60.7
Glu97(B), O <sup>ε1</sup>	Thr75(A), O <sup>γ1</sup>	99.9	5
Arg98(B), N <sup>η1</sup>	Thr75(A), O	99	-
Asn10(B), N <sup>δ2</sup>	Thr75(A), O <sup>γ1</sup>	76	29.8
Gly76(A), N	Gln64(B), O <sup>ε1</sup>	98.2	32.1
Arg98(B), N <sup>η1</sup>	Glu77(A), O <sup>ε1</sup>	88.8	-
Arg98(B), N <sup>η2</sup>	Glu77(A), O <sup>ε1</sup>	78.12	-
Leu17(B), N	Asp85(A), O <sup>δ1</sup>	75.4	31.8

(A) denotes subunit A

(B) denotes subunit B

hydrogen bonding stability of native hydrogen bonds between the unmodified PfTIM and PfTIMC13(A)-SSG. Table 5 shows the list of non-native hydrogen bonding donor and acceptor pairs formed during the course of simulations. From the percentage occurrences listed in Table 5 one can infer that the pattern of non-native hydrogen bonding is predominantly different across the trajectories for the unmodified PfTIM and PfTIMC13(A)-SSG.

**Table 5**  
MD statistics of nonnative inter-subunit donor-acceptor pairs of hydrogen bonds.

Donor atoms	Acceptor atoms	% occurrence in PfTIM	% occurrence in PfTIMC13 (A)-SSG
Lys12 (A), N <sup>c</sup>	Gly72 (B), O	31.2	-
Lys12 (A), N <sup>c</sup>	Ser73 (B), O <sup>y</sup>	6.3	23.0
Cys13 (A), N	Asn69 (B), O <sup>δ1</sup>	52.8	-
Asn71 (A), N <sup>δ2</sup>	Gly15 (B), O	36.4	1.7
Lys12 (B), N <sup>c</sup>	Ser73 (A), O <sup>y</sup>	20.0	21.3
Thr75 (A), N	Glu97 (B), O <sup>ε2</sup>	98.2	0.4
His47 (A), N <sup>ε2</sup>	Asp85 (B), O <sup>δ1</sup>	3.03	27.4

(A) denotes subunit A

(B) denotes subunit B

The intersubunit distance separation between the C<sup>α</sup> - C<sup>α</sup> atoms of Ser45 (A) and Ser45 (B) for PfTIMC13(A)-SSG starts to increase at the end of the simulation indicating weakening of dimer stability. Glutathionylation of Cys13 disturbs the inter-subunit hydrogen bond interactions. The structural perturbation of the dimeric interface loops caused by Cys13 glutathionylation gives rise to an entrance for water molecules into the dimer interface (Figure 5). The NACCESS scan for these trajectories are in agreement with the observed results suggesting that the dimer stability is challenged as a result of glutathionylation at Cys13 of TIM.

#### Changes in Lys12 active site geometry

Lys12 residue plays a very crucial role in binding, catalysis and chemistry in TIM. Various stabilizing interactions with nearby residues like His95, Glu97 from the same subunit and Ser73 from the other subunit help to maintain the bound conformation of Lys12. The changes in geometry

of Lys12 was tracked during the simulation runs by monitoring the distance between Lys12 side chain N<sup>c</sup> atom and the sidechain carboxyl atom of Glu97 and the sidechain N<sup>e</sup> atom of His95. It is evident from the plots in Figure 6 that the environment around Lys12 undergoes significant changes at the end of the simulation for PfTIMC13(A)-SSG indicating distorted active site geometry. The pseudodihedral angle plots for the considered residues suggest that the deviation is largely due to side-chain motion which distorts the active site geometry of the enzyme when Cys13 gets glutathionylated. Loss of local stabilizing interactions at the interface of the dimer due to glutathionylation of Cys13 may decrease the energy barrier of Lys12 structural transition

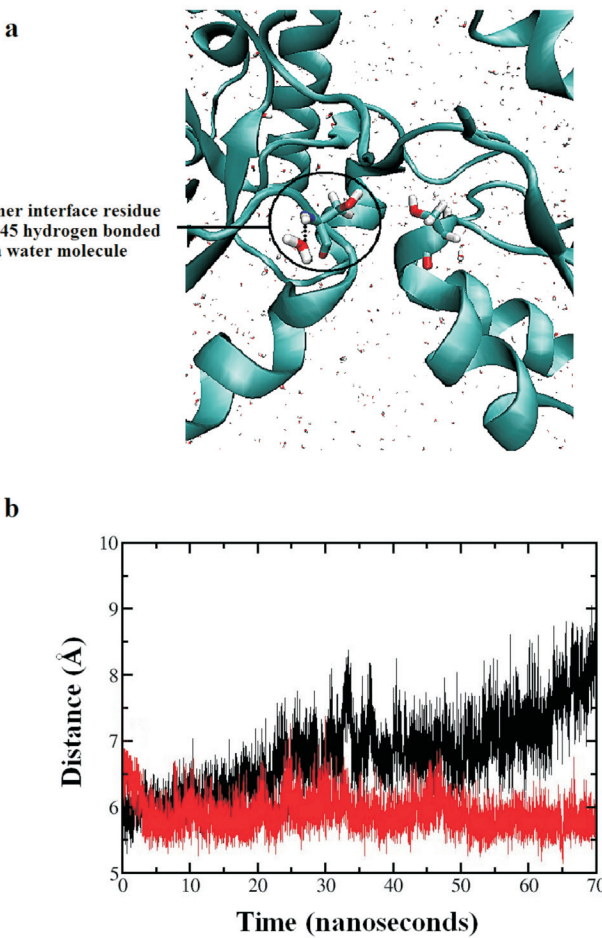


**Figure 5: Weakening of Dimer interface Stability**

- A snapshot of PfTIMC13(A)-SSG taken at 70ns showing water molecule hydrogen bonded to interface residue Ser45 (A).
- Distance between the C<sup>α</sup> - C<sup>α</sup> atoms of dimer interface residues Ser45 (A) and Ser45 (B) along the 70ns trajectories of PfTIM (red) and PfTIMC13(A)-SSG (black).

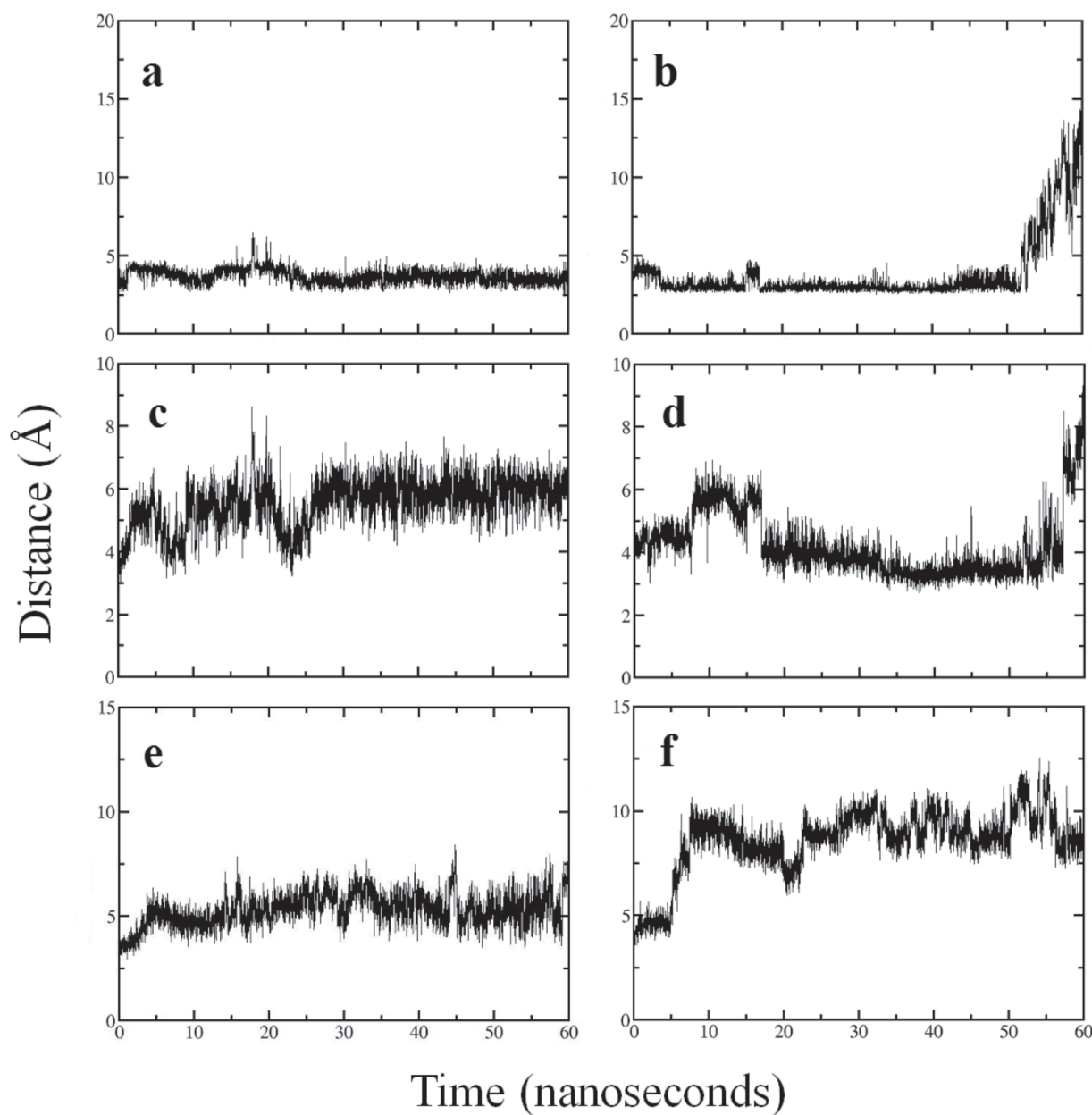


**Figure 6: Distances between select atoms in close proximity to the active site residue Lys12 side chain as function of time:**

Plots a and b indicate the distance between side chain N<sup>ε</sup> atom of Lys12 to side chain O<sup>δ2</sup> atom of Glu97 (subunit A) for PftIM and PftIMC13(A)-SSG respectively.

Plots c and d indicate the distance between side chain N<sup>ε</sup> atom of Lys12 to side chain N<sup>δ2</sup> atom of His95 (subunit A) for PftIM and PftIMC13(A)-SSG respectively.

Plots e and f indicate the distance between side chain N<sup>ε</sup> atom of Lys12 to side chain N<sup>δ2</sup> atom of His95 (subunit B) for PftIM and PftIMC13(A)-SSG respectively.

leading to destabilization of catalytically active Lys12 conformation.

All the structural changes reported in the results section have been observed in multiple simulations of PftIMC13(A)-SSG and PftIMC217(A)-SSG.

## Discussion

Triose-phosphate isomerases are structurally conserved across species and are known to be catalytically active only in their homodimeric form. The interface across the subunits is stabilized by a number of polar and non polar

interactions involving loop 1 residues from one subunit to the loop 3 residues from the other subunit. In the case of PfTIM, Cys13 in loop 1 forms a number of interactions with loop 3 residues involving the backbone of Phe69, Asn71, Gly72, Ser73, Tyr74 and Glu77 of the other subunit. Further Cys13 is also involved in side chain-side chain interactions with Ser67, Glu77 and Ser79.

Cys13 which has only limited solvent accessibility in the native dimeric structure undergoes rapid modification with thiolating agents and contributes to enzyme inhibition. The high rate of labeling of this residue may be due to its low pKa, loop dynamics and possibly from electrostatic steering of negatively charged glutathione towards the positively charged surface surrounding the active site. Mass spectrometric studies done in my lab had shown that the glutathione labeling kinetics of PfTIM closely corresponds with the iodoacetamide labeling of PfTIM reported from a previous study (Maithal *et al.*, 2002).

A similar loss in enzymatic activity on derivatization of the interface cysteine with the sulphydryl reagent methyl methanethiosulfonate has been reported from other parasitic TIMs from *T.brucei*, *T.cruzi*, and *L.mexicana* (Perez-Montfort *et al.*, 1999). In a previous study involving the subunit interface mutant Y74G distinct peaks corresponding to both dimeric and monomeric species have been observed (Maithal *et al.*, 2002).

MD simulations reveal the structural effects of S-Glutathionylation of Cys-13 present in the dimer interface and give insights into the inactivation of the enzyme. The dimer stability of TIM is seriously challenged by S-Glutathionylation of Cys-13 and leads to inactive conformational states of catalytic residue Lys-12. Reactivation of Cys13 labeled wild type PfTIM was not possible because spontaneous reassociation of monomers does not happen after deglutathionylation under dilute *in vitro* conditions and may also be indicative of some level of unfolding.

The complete reversibility of activity by glutathionylation/deglutathionylation of Cys217 reinforces the potential significance of allosteric

modulation of activity through this residue (Hameed *et al.*, 2012). Cys217 situated at the N-terminal of Helix G has been shown to frequently undergo helix transitioning between  $\alpha$  to  $3_{10}$  forms in the presence of substrate. In Glycerol-3-phosphate bound yeast TIM, residues at the N-termini and C-termini of helix G – Asn213, Phe220 and Lys221 were found to have  $^{15}\text{N}$  chemical exchange rate constants ( $R_{\text{ex}}$ ) significantly above zero indicative of slow conformational exchange process on the *is-ms* time scales (Massi *et al.*, 2006). Recently it has been shown that residues in helix-G are involved in protein-protein interactions with redox proteins like thioredoxin (Hameed *et al.*, 2012). The dynamic nature of redox interactomes requires fast and transient molecular switches and therefore the underlying recognition motifs are usually short segments that are structurally malleable. Recognition through linear motifs results in interactions with iM affinities that underlie transient, reversible complexes, adapted for effective regulation. They also serve as consensus sites of post-translational modification and recognition elements in transient complexes (Joseph *et al.*, 1990).

MD simulations reveal the structural effects of S-glutathionylation of Cys-217 present in Helix G and provide an explanation for enzyme inactivation. Though the overall structure of TIM is not significantly perturbed by S-glutathionylation of Cys-217, as seen from global  $C_{\alpha}$  based RMSD plots, Helix G undergoes significant structural change and is reduced to a short  $3_{10}$  helix during the simulations. The N-terminal residues of Helix G take up coil conformations.

The hydrogen bonding statistics of the simulation run predict that loop 6, the catalytic loop of TIM, may lose stability and can become disordered. Loop 6 consists of 11 residues, which can be divided into a three residue N-terminal hinge, a five residue rigid tip of the loop and a three residue C-terminal hinge. It is a well established fact that loop-6 plays a very crucial role in the catalysis of triose-phosphate isomerase. The loop can assume two different conformations: open, leaving the active site accessible to the solvent and substrate, and closed, blocking the entrance to the active site and preventing the loss

of the reaction intermediate. The loop has been hypothesized to move as a rigid body because structural changes between open and closed conformations are localized to the hinge residues (Wang *et al.*, 2009). In the ligand bound closed form the Gly171 at the tip of the loop makes a hydrogen bond with its amide nitrogen to the phosphate moiety of the bound ligand. Interactions between loop 6 and loop 7 (residues 208 - 212) are necessary to provide the proper chemical environment for the reaction to occur and the interactions play a significant role in modulating active site dynamics (Pompliano *et al.*, 1990). Deletion mutant studies on loop 6 have indicated that enzyme activity gets drastically affected, because of loss of the enediol intermediate, upon mutation of loop 6 residues (Flores *et al.*, 2011). The MD simulations reported in this manuscript predict that glutathionylation of Cys217 may allosterically induce loop 6 disorder. This may interfere with its natural rigid body hinge type motion and its reaction-intermediate stabilizing role and will lead to abolition of enzyme activity.

Further MD studies predict that ligand dissociation can be enhanced upon Cys-217 glutathionylation due to high amplitude motions involving phosphate binding loops. This offers an explanation for the high  $K_m$  values reported for Cys-217 derivatized TIM. The mechanism of inhibition by glutathionylation of Cys-217 appears purely kinetic and therefore can be readily reversed by deglutathionylation. However there was no loss of activity when C13E mutant PfTIM was treated with IAM. This means that carboxy-methylation of Cys-217 does not render the enzyme inactive while glutathionylation of Cys-217 renders the enzyme inactive. In previous studies it has been shown that although Cys217 does not form part of the catalytic site, its transformation to a phenyl disulfide exerts important effects on the kinetics of the enzyme (Garza-Ramos *et al.*, 1996). This suggests that modification of Cys-217 with bulky thiol reagents renders the enzyme inactive. It has been shown in *Giardia lamblia* TIM that derivatization of Cys222 (equivalent to Cys217 of PfTIM) significantly decreased the affinity for the substrate (Ginsburg *et al.*, 2010) and led to very high  $K_m$ . Reversibility by DTT of S-phenyl-p-

toluenethiosulfonate action in other TIMs that have a Cys217 has been observed.

Thus it is clear that S-glutathionylation can cause reversible allosteric inhibition of TIMs that lack Cys13, but otherwise have Cys217; those that lack Cys13 and Cys217 will be hardly affected by S-glutathionylation.

The fact that glutathionylation of Cys217 leads to loss of activity is interesting as in mammalian TIM Cys217 is conserved and further human TIM has methionine instead of Cys13. This may be very interesting as regulation of human TIM by reversible glutathionylation of Cys217 may have implications in cancer. There are many parallels that can be drawn between malarial parasites and tumour cells (Zhang *et al.*, 1987; Ginsburg *et al.*, 2010). Both of them are heavily dependent upon glycolysis for their energy requirements and avoid mitochondrial respiration as a source of energy (Warburg effect). This may help to prevent oxidative stress to some extent as mitochondrial respiratory chain is a powerful source of reactive oxygen species. Both *Plasmodium falciparum* and tumor cells are particularly susceptible to oxidative challenge and thiol based redox systems involving glutathione system and the thioredoxin system play crucial roles in antioxidant defense. Drugs which target thiol based redox enzymes and glutathione metabolism would cripple the antioxidant defense system of the parasite/tumor cell and would lead to widespread inhibition of many target enzymes involved in various processes of metabolism.

Further it has been shown in T-lymphocytes that human TIM, which possess Cys-217 but lacks dimeric interface cysteine, is a target of S-glutathionylation during oxidative stress conditions (Fratelli *et al.*, 2002). Thus glutathionylation/deglutathionylation of Cys-217 could effectively regulate the activity of TIM and provides a novel mechanism whereby ROS/RNS can modulate S-glutathionylation and regulate this key glycolytic enzyme.

## Conclusion

This computational study predicts how S-glutathionylation of Cys217 results in allosteric inhibition of TIM. This study leads to the conclusion that homologous TIMs that lack Cys-

13 but have Cys-217 can potentially be regulated by ROS/RNS via S-glutathionylation through reversible allosteric modulation of enzyme activity. This may constitute a novel mechanism of redox regulation of Triosephosphate isomerase.

### Acknowledgements

MSSH would like to thank Prof.Siddhartha P. Sarma, Molecular Biophysics Unit, Indian Institute of Science for his valuable discussion during the manuscript preparation. MSSH would like to acknowledge DBT and DST for funding the computing facilities.

### Abbreviations

TIM, Triosephosphate isomerase; PfTIM, *Plasmodium falciparum* Triosephosphate isomerase; PfTIMC13(A)-SSG, *Plasmodium falciparum* Triosephosphate isomerase *in silico* glutathionylated at Cys13 in subunit A; PfTIMC217(A)-SSG, *Plasmodium falciparum* Triosephosphate isomerase *in silico* glutathionylated at Cys217 in subunit A; RMSD, root-mean square deviation; MD, Molecular dynamics; TCA, Tricarboxylic acid; DHAP, Dihydroxy acetone phosphate; G3P, Glyceraldehyde-3-phosphate; ATP, Adenosine triphosphate; GSH, reduced glutathione; GSSG, oxidized glutathione; ns, nanoseconds; ps, picoseconds.

### References

- Albery, J. and Knowles, J. R. (1976). Free-energy profile of the reaction catalyzed by triosephosphate isomerase. *Biochemistry* 15, 5631–5640.
- Brandes, N., Schmitt, S. and Jakob, U. (2009). Thiol-based redox switches in eukaryotic proteins. *Antioxid Redox Signal*. 11, 997–1014.
- Cooper, A.J., Pinto, J.T. and Callery, P.S. (2011). Reversible and irreversible protein glutathionylation: biological and clinical aspects. *Expert Opin Drug Metab Toxicol*. 7, 891–910. Erratum in: *Expert Opin Drug Metab Toxicol*. 7, 1183.
- Cotgreave, I.A., Gerdes, R., Schuppe-Koistinen, I. and Lind, C. (2002). S-glutathionylation of glyceraldehyde-3-phosphate dehydrogenase: role of thiol oxidation and catalysis by glutaredoxin. *Methods Enzymol.* 348, 175–182.
- Cui, Q. and Karplus, M. (2002). Quantum mechanics/molecular mechanics studies of triosephosphate isomerase-catalyzed reactions: effect of geometry and tunneling on proton transfer rate constants. *J Am Chem Soc* 24, 3093–3124.
- Dalle-Donne, I., Rossi, R., Colombo, G., Giustarini, D. and Milzani, A. (2009). Protein S-glutathionylation: a regulatory device from bacteria to humans. *Trends Biochem Sci*. 34, 85–96. D'Autréaux, B. and Toledano, M.B. (2007). ROS as signaling molecules: mechanisms that generate specificity in ROS homeostasis. *Nat Rev Mol Cell Biol*. 8, 813–824.
- Flores, S.E., Romero, A.R., Alca'ntara, G. H., Hernández, J.O., Castrello, G.P., Hernández, G.P., Mora, I., Villanueva, A.C., Torres, I.G., Me'ndez, S.T., Manzo, S.G., Arroyo, A.T., Vela'zquez, G.L. and Vivas H.R. (2011). Determining the molecular mechanism of inactivation by chemical modification of triosephosphate isomerase from the human parasite Giardia lamblia: A study for antiparasitic drug design. *Proteins* 79, 2711–2724.
- Foster, M.W., Hess, D.T. and Stamler, J.S. (2009). Protein S-nitrosylation in health and disease: a current perspective. *Trends Mol Med*. 15, 391–404.
- Fratelli, M., Demol, H., Puype, M., Casagrande, S., Eberini, I., Salmona, M., Bonetto, V., Mengozzi, M., Duffieux, F., Miclet, E., Bach, A., Vandekerckhove, J., Gianazza, E. and Ghezzi, P. (2002). Identification by redox proteomics of glutathionylated proteins in oxidatively stressed human T lymphocytes. *Proc Natl Acad Sci*. 99, 3505 – 3510.
- Garza-Ramos, G., Perez-Montfort, R., Rojo-Dominguez, A., de Gomez-Puyou, M.T. and Gomez-Puyou, A. (1996). Species-specific inhibition of flogous enzymes by modification of non-conserved amino acid residues. The cysteine residues of triosephosphate isomerase, *Eur J Biochem*. 241, 114–120.
- Ghezzi, P., Bonetto, V. and Fratelli, M. (2005). Thiol/Disulfide Balance: From the Concept of Oxidative Stress to that of Redox Regulation, *Antioxid Redox Signal* 7, 964–972.
- Ginsburg, H. (2010). Malaria parasite stands out, *Nature*. 466, 702–703.
- Hameed, M. S. S. and Sarma, S. P. (2012). The Structure of the Thioredoxin-Triosephosphate Isomerase Complex Provides Insights into the Reversible Glutathione-Mediated Regulation of Triosephosphate Isomerase. *Biochemistry*. 51, 533–544.
- Ito, H., Iwabuchi, M. and Ogawa, K. (2003). The SugarMetabolic enzymes Aldolase and triosephosphate isomerase are targets of glutathionylation in *Arabidopsis thaliana*: Detection using biotinylated glutathione. *Plant Cell Physiol* 44, 655–660.
- Joseph, D., Petsko, G. A. and Karplus, M. (1990). Anatomy of a conformational change: hinged “lid” motion of the triosephosphate isomerase loop, *Science* 249, 1425–1428.
- Kiley, P.J. and Storz, G. (2004). Exploiting thiol modifications. *PLoS Biol*. 2:e400.
- Klatt, P., and Lamas, S. (2000). Regulation of protein function by S-glutathiolation in response to oxidative and nitrosative stress. *Eur. J. Biochem*. 267, 4928–4944.
- Knowles, J. R. (1991). Enzyme catalysis, not different, just better. *Nature* 350, 121–124.
- Kumsta, C. and Jakob, U. (2009). Redox-regulated chaperones. *Biochemistry*. 48, 4666–76.
- Kurkcuoglu, O., Jernigan, R.L. and Dorucker, P. (2006). Loop motions of triosephosphate isomerase observed with elastic networks. *Biochemistry*, 45, 1173–1182.
- Lee, B. and Richards, F. M. (1971). The interpretation of protein structures: estimation of static accessibility. *J. Mol. Biol.* 55, 379 – 400.

- Leitner, M., Vandelle, E., Gaupels, F., Bellin, D. and Delledonne, M. (2009). NO signals in the haze: nitric oxide signalling in plant defence. *Curr. Opin. Plant Biol.* 12, 451–458.
- Maithal, K., Ravindra, G., Balaram, H. and Balaram, P. (2002). Inhibition of Plasmodium falciparum Triosephosphate isomerase by chemical modification of an Interface Cysteine. Electrospray ionization mass spectrometric analysis of differential cysteine reactivities. *J. Biol. Chem.* 277, 25106-25114.
- Maithal, K., Ravindra, G., Nagaraj, G., Singh, S.K., Balaram, H. and Balaram, P. (2002). Subunit interface mutation disrupting an aromatic cluster in Plasmodium falciparum triosephosphate isomerase: effect on dimer stability. *Protein Eng. Des. Sel.* 15, 575 – 584.
- Marino, S.M., Li, Y., Fomenko, D., Agisheva, N., Cerny, R.L. and Gladyshev, V.N. (2010). Characterization of surface-exposed reactive cysteine residues in *Saccharomyces cerevisiae*. *Biochemistry* 49, 7709–7721.
- Massi, F., Wang, C. and Palmer, A.G. (2006). Solution NMR and Computer simulation studies of active site loop motion in Triosephosphate isomerase. *Biochemistry* 45, 10787 – 10794.
- Michelet, L., Zaffagnini, M., Massot, V., Keryer, E., Vanacker, H., Miginiac-Maslow, M., IssakidisBourgues, E., and Lemaire D.S. (2006). Thioredoxins, glutaredoxins and glutathionylation: new crosstalks to explore. *Photosynth Res.* 89, 225-245.
- Mieyal, J.J. and Chock P.B. (2012). Posttranslational modification of cysteine in redox signaling and oxidative stress: focus on S-glutathionylation. *Antioxid Redox Signal.* 16, 471-475.
- Mohr, S., Hallak, H., de Boitte, A., Lapetina, E.G. and Brüne, B. (1999). Nitric oxide-induced S-glutathionylation and inactivation of glyceraldehyde-3-phosphate dehydrogenase. *J. Biol. Chem.* 274, 9427-9430.
- Nakamura, H., Nakamura, K. and Yodoi, J. (1997). Redox regulation of cellular activation. *Annu Rev Immunol.* 15, 351–369.
- Parthasarathy, S., Ravindra, G., Balaram, H., Balaram, P. and Murthy, M. R.N. (2002). Structure of the Plasmodium falciparum Triosephosphate Isomerase Phosphoglycolate Complex in two crystal forms, Characterization of Catalytic loop open and closed Conformations in the Ligand-Bound State, *Biochemistry* 41, 13178-13188.
- Pérez-Montfort, R., Garza-Ramos, G., Alcántara, G.H., Reyes-Vivas, H., Gao, X., Maldonado, E., GómezPuyou, M. and Gómez-Puyou, A. (1999). Derivatization of the Interface Cysteine of Triosephosphate Isomerase from *Trypanosoma brucei* and *Trypanosoma cruzi* as Probe of the Interrelationship between the Catalytic Sites and the Dimer Interface. *Biochemistry* 38, 4114–4120.
- Pompliano, D. L., Peyman, A. and Knowles, J. R. (1990). Stabilization of a reaction intermediate as a catalytic device: definition of the functional-role of the flexible loop in triosephosphate isomerase, *Biochemistry* 29, 3186-3194.
- Reddie, K.G. and Carroll, K.S. (2008). Expanding the functional diversity of proteins through cysteine oxidation. *Curr Opin Chem Biol* 12, 746–754.
- Rhee, S.G., Kang, S.W., Jeong, W., Chang, T.S., Yang, K.S. and Woo, H.A. (2005). Intracellular messenger function of hydrogen peroxide and its regulation by peroxiredoxins. *Curr Opin Cell Biol* 17, 183–189.
- Rosovsky, S., Joel, G., Tong, L. and McDermott, A.E. (2001). Solution-state NMR investigations of triosephosphate isomerase active site loop motion: ligand release in relation to active site loop dynamics. *J. Mol. Biol* 310, 271–280.
- Waley, S.G. (1973). Refolding of triosephosphate isomerase. *Biochem J.* 135, 165–172.
- Wang, Y., Berlow, R.B. and Loria, J.P. (2009). The role of Loop-Loop interactions in Coordinating Motions and Enzymatic function in Triosephosphate Isomerase, *Biochemistry* 48, 4548-4556.
- Xiong, Y., Uys, J.D., Tew, K.D. and Townsend, D.M. (2011). S-glutathionylation: from molecular mechanisms to health outcomes. *Antioxid Redox Signal.* 15, 233-270.
- Zabori, S., Rudolph, R. and Jaenicke, R. (1980). Folding and association of triosephosphate isomerase from rabbit muscle. *Z Naturforsch* 35, 999–1004.
- Zomosa-Signoret, Mason, I.F., Hernández-Alcántara, G., Reyes-Vivas, H., Martínez-Martínez, E. and GarzaRamos, G. (2003). Control of the reactivation kinetics of homodimeric triosephosphate isomerase from unfolded monomer. *Biochemistry* 42, 3311–3318.
- Zhang, Y. (1987). Malaria: an intra-erythrocytic neoplasm? *Parasitology Today.* 3, 190-192.